IOP Conf. Series: Materials Science and Engineering **719** (2020) 012039 doi:10.1088/1757-899X/719/1/012039

# Research on Mutual Inductance Prediction of Resonant Magnetic Coupling Wireless Power Transmission System Based on Recursive Least Square Method

**Songcen Wang[1], Bin Wei[1], Hao He[1], Jianxue Mu[2] and Changsong Cai[2]**

1China Electric Power Research Institute, Beijing, China
2School of Electrical Engineering and Automation, Wuhan University, Wuhan, Hubei Province, China.
Email: 1071831864@qq.com

**Abstract.** In this paper, based on recursive least square algorithm and resonant magnetic coupling wireless power transmission technology, the magnetic coupling mutual inductance value, which is a significant factor affecting the transmission power and efficiency of wireless transmission system, is predicted. According to the characteristics of the system, a mathematical model of LCC-P-type topology structure is established. Through mathematical deduction and analysis, combined with MATLAB/Simulink simulation results are obtained, and its feasibility is verified by experimental results.

## 1. Introduction

Wireless Power Transmission (WPT) is a technology that can obtain electric power without direct contact.

The resonant magnetic coupling (RMC) WPT studied in this paper is a hot way of WPT at present. Because of its high efficiency, long distance, low loss, low radiation, selective transmission and other advantages, this method has been widely applied in the field of WPT. In the RMC WPT system, monitoring of transmission status can greatly ensure the safe operation and coordinated control of the system. However, the detection process is cumbersome and the cost is high. Therefore, the purpose of this paper is to find out the key electrical parameters of the primary side which can reflect the overall parameters of the system by studying the equivalent circuit model of the RMC WPT system, and finally realize the monitoring of the electrical parameters of the RMC WPT device measurement.

## 2. WPT System Based on LCC-P Topology

### *2.1. Selection of Topological Structure*

Generally, RMC WPT systems have five typical topologies: SS-type topology, SP-type topology, PS-type topology, PP-type topology and LCC-P-type topology. In practical experiments, it is found that when the frequency of the WPT system is close to the resonant frequency, the series (S) structure will lead to a large primary current, which is often unable to work at the resonant frequency. The LCC-P-type topology, because of the existence of series inductance $L_3$, can produce stable power transfer even if the coil deviates or the load changes. It generates a constant current in the transmission coil [1], so that the current in the transmission coil does not rise very much. Therefore, it can make the WPT system work at a frequency that is very close to the resonance point, and in the theoretical calculation, it can also produce stable power transfer. It can be assumed that the system works in a fully resonant

state, which greatly simplifies the theoretical calculation. Therefore, this paper takes the WPT system with LCC-P topology as an example for structural analysis.

The equivalent circuit model of WPT system with LCC-P-type topology is shown in figure 1. $u_p$ is a high frequency AC voltage source. $L_1$, $C_1$, $L_3$, $C_3$, $L_2$ and $C_2$ constitute primary and secondary side resonance networks respectively. $R_1$, $R_2$ and $R_3$ are the internal resistances of $L_1$, $L_2$ and $L_3$ respectively (because the conductance of capacitors is very small, the influence of capacitance conductance on the model is neglected here). $M$ is the mutual inductance between primary and secondary coils. $R_L$ is the load resistor that is connected to simulate the charging of different types of wireless charging devices in the resonant circuit. $I_1$ and $I_2$ are the primary and secondary side high frequency resonance current, respectively.

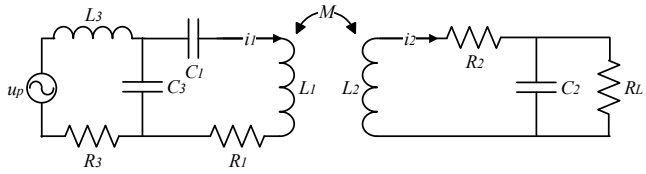


**Figure 1.** The equivalent circuit model of WPT system with LCC-P-type topology

*2.2. Mapping Relation of Electrical Parameters between Primary Side and Secondary Side*

Before theoretical analysis, some assumptions need to be made:

1) Circuit parameters $L_1$, $L_2$, $L_3$, $C_1$, $C_2$, $C_3$, $R_1$, $R_2$ and $R_3$ are known quantities measured.

2) Under normal operating conditions, these circuit parameters do not change much, so they are generally considered constant [2-3].

3) The internal resistance $R_1$, $R_2$ and $R_3$ of the coil inductances $L_1$, $L_2$ and $L_3$ of the primary and secondary sides are very small relative to the inductance value, and their influence on the resonance frequency can be neglected. When the system works in the full resonance state, it can be considered that the frequency of the high frequency AC voltage (the frequency used in the WPT system in this study is about 300 kHz) is satisfied

$$f=\frac{1}{2\pi\sqrt{L_1C_1}}=\frac{1}{2\pi\sqrt{L_2C_2}}=\frac{1}{2\pi\sqrt{L_3C_3}} \tag{1}$$

After the above hypothesis analysis, in the equivalent circuit model of the new LCC-P topology, the $L_1$ and $C_1$, $L_3$ and $C_3$ of the primary side are fully resonant, while the $L_2$ and $C_2$ of the secondary side are fully resonant. The theoretical analysis based on this is as follows.

In this WPT system, if the effective value phasor of high frequency AC voltage $u_p$ is set to $\dot{U}_p = U_p\angle 0°$, that is, the effective value of $u_p$ is $U_p$, and the initial phase angle is 0°, the loop equation can be formulated according to the equivalent circuit model

$$\begin{cases}(R_1+R_3)\dot{I}_1-j\omega M\cdot\dot{I}_2=\dot{U}_p\\ -j\omega M\cdot\dot{I}_1+(R_2+R_L)\dot{I}_2=0\end{cases} \tag{2}$$

Among them, $\dot{I}_1$ and $\dot{I}_2$ are the effective phasors of the primary and secondary AC currents $i_1$ and $i_2$ respectively.

Solute the (2) equation yields a current parameter expression of the follows for the primary side and the secondary side:

$$\begin{cases} \dot{I}_1 = \dfrac{R_2 + R_L}{\omega^2 M^2 + (R_1 + R_3)(R_2 + R_L)} \dot{U}_p \\ \dot{I}_2 = \dfrac{j\omega M}{\omega^2 M^2 + (R_1 + R_3)(R_2 + R_L)} \dot{U}_p \end{cases} \tag{3}$$

From the deduction of formula (2) ~ (3), it can be seen that the current parameters of the primary and secondary sides are not only related to the parameters of WPT system itself, but also to the high frequency AC voltage. However, the key electrical parameters of the primary side, which can reflect the overall parameters of the system, should not change with the change of high frequency AC voltage, so these parameters are not the key electrical parameters we are looking for. In the next section, we will look for the primary key electrical parameters that can reflect the overall parameters of the system.

*2.3. Key Electrical Parameters of Primary Side*

In the actual experiment, the high frequency AC voltage is realized by inverters. The circuit structure is shown in figure 2. $U_d$ is the input DC voltage of the primary side, $C_d$ is the large capacitor parallel to $U_d$, $S_1$~$S_4$ is the full bridge inverter, $D_1$~$D_4$ is the feedback diode (or continuous current diode), and $u_p$ is the equivalent input voltage of the resonant circuit, that is, the resonant circuit.

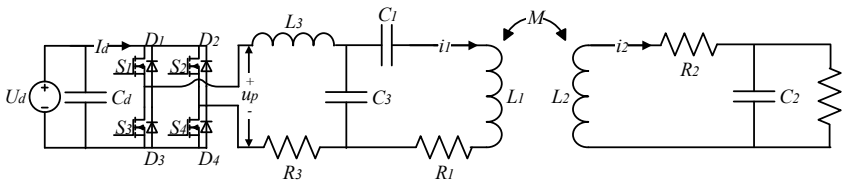


**Figure 2.** LCC-P-type Topological Equivalent Circuit Model with Inverter

When the phase difference between positive and negative voltage of $u_p$ is 180°, the Fourier series expansion shows that the fundamental effective value of high frequency AC voltage on the primary side has the following quantitative relationship with the primary input DC voltage $U_d$:

$$U_d = \frac{\sqrt{2}\pi}{4} U_p \tag{4}$$

According to the law of conservation of power, the input power of the inverters should be equal to the output power, ignoring the power loss caused by the inverters. From this we can get:

$$I_d = \frac{2\sqrt{2}}{\pi} I_1 \tag{5}$$

Because the WPT system is in full resonance state at this time, and the dimension of $\dfrac{\omega^2 M^2 + (R_1 + R_3)(R_2 + R_L)}{R_2 + R_L}$ is Ohm (Ω), i.e. $\dot{U}_p$ and $\dot{I}_1$ are in phase, the relationship between DC voltage $U_d$ and current $I_d$ can be obtained by combining formula (3), (4) and (5):

$$U_d = \frac{\pi^2}{8} \cdot \frac{\omega^2 M^2 + (R_1 + R_3)(R_2 + R_L)}{R_2 + R_L} I_d \tag{6}$$

Let $R_d = \frac{U_d}{I_d}$, which is called the equivalent input resistance on the DC side, therefore, $M$ can be represented by $R_d$ and $R_L$ as follows:

$$M = \frac{\sqrt{(\frac{8}{\pi^2} R_d - R_1 - R_3)(R_2 + R_L)}}{\omega} \tag{7}$$

In the above formula, $R_d$ is not affected by the high frequency AC voltage. It is the key electrical parameter of the primary side required. The load $R_L$ can be directly known by wireless frequency identification technology [4]. So only $M$ cannot be measured directly from the primary side.
In the follow-up simulation and experiment, because of the inevitable error, $M$ obtained each time is not the real value, which need to be measured repeatedly through a large number of experiments. By changing the phase difference between the two control signals, a series of comparative experiments can be obtained, so that a series of $M$ can be obtained in different ways. A large amount of data measured by the above experiments can be processed by recursive least square (RLS) algorithm.
When the phase difference of the two control signals is adjusted to change, for example, when it is set to be $\theta$, formula (7) will be expressed as follows:

$$M = \frac{\sqrt{[\frac{4(1-\cos\theta)}{\pi^2} R_d^* - R_1 - R_3][R_2 + R_L]}}{\omega} \tag{8}$$

The $R_d$* is the equivalent input resistance of the DC side measured in the case of the corresponding phase difference $\theta$.

## 3. Simulation Design Based on RLS Algorithms

### *3.1. WPT System Simulation Design*

A WPT system with LCC-P topology is built on Simulink interface. The simulation wiring is shown in figure 3, and the parameters of the components are shown in table 1.

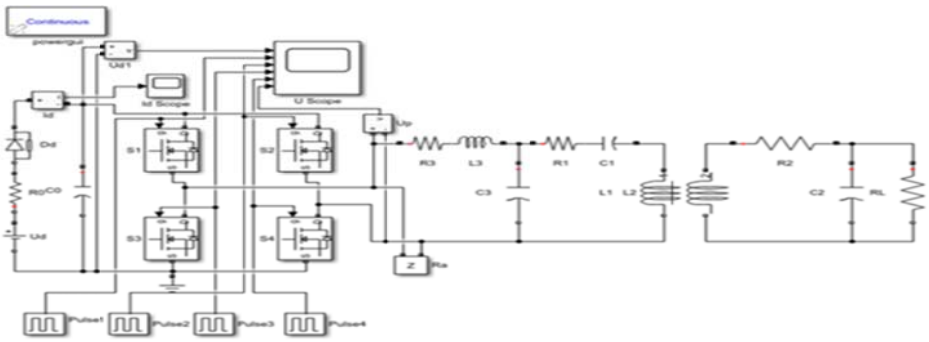

**Figure 3.** WPT System Simulation Wiring Diagram of LCC-P Topology

**Table 1.** Component Parameters of Simulation System

| **Component Number** | $U_d$ | $R_0$ | $C_0$ | $L_1$ | $L_2$ | $L_3$ | $C_1$ |
|---|---|---|---|---|---|---|---|
| **Parameter Values** | 12V or 24V | 0.00001Ω | 1mF | 112μH | 14.4525μH | 6μH | 2.513nF |
| **Component Number** | $C_2$ | $C_3$ | $R_1$ | $R_2$ | $R_3$ | $R_L$ | $M$ |
| **Parameter Values** | 19.474nF | 46.9nF | 1.55Ω | 0.2Ω | 0.083Ω | 50Ω or 25Ω | 8.5μH |

From the above table, the coefficient of *M* of primary side and secondary side is set at 8.5 μH. The simulation results show that the value fluctuates from 8 μH to 9 μH with an average of 8.57 μH.

*3.2. RLS Algorithm*

The RLS parameter identification is that when the recognition system runs, with the introduction of new recursive observation data, the parameters are estimated one after another until the estimated value reaches satisfactory accuracy. The basic idea of RLS algorithm can be summarized as follows: the new parameter value to be estimated $\hat{\theta}(k)$ = the old parameter value to be estimated $\hat{\theta}(k-1)$ + the correction term [5].

The comparison of the recursive value of *M* and the stability value of *M* is shown in figure 4.

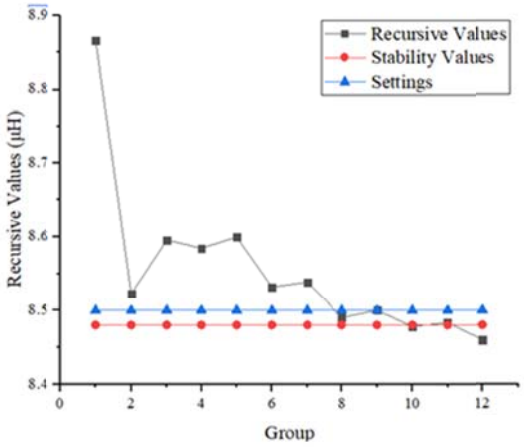


**Figure 4.** Comparisons among Recursive Values, Stable Values and Settings of Mutual Inductance

From figure 4, it can be seen that after 8 recursions, the *M* is almost completely stable around 8.48 μH, which shows that the convergence speed of the RLS algorithm is very fast.

According to the results of the above simulation combined with the algorithm, the *M* is about 8.48 μH, while the actual *M* set in the simulation experiment is 8.50 μH, the error is about 0.2353%, which is much smaller than the average value error. Through simulation and RLS algorithm, this method can detect the mutual inductance between coils only by measuring the DC side voltage and current of the primary side, which is feasible and has high accuracy.

## 4. Physical Construction and Actual Measurement

In order to verify the feasibility of the design of the parameter sampling and control circuit in Chapter 3, a practical WPT system circuit is made, as shown in figure 5.

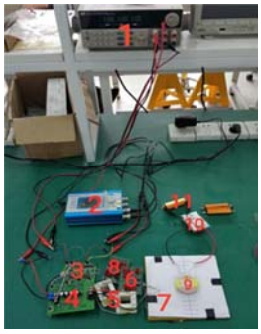

**Figure 5.** WPT System Circuit

Among them, label 1 is power supply, 2 is control signal generator, 3 is drive circuit board, 4 is inverted circuit board, 5 is inductor $L_3$ and its internal resistance $R_3$, 6 is primary capacitor $C_3$, 7 is primary coil $L_1$, 8 is primary capacitor $C_1$, 9 is secondary coil $L_2$, 10 is secondary capacitor $C_2$, 11 is load resistance $R_L$.
The parameters of the components used in the experiment are as shown in table 2.

**Table 2. Parameters of Components Used in Experiments**

| **Component Number** | $U_d$ | $L_1$ | $L_2$ | $L_3$ | $C_1$ | $C_2$ |
|---|---|---|---|---|---|---|
| **Parameter Values** | 12V or 24V | 126.46μH | 14.41μH | 6.112μH | 2.1618nF | 19.537nF |
| **Component Number** | $C_3$ | $R_1$ | $R_2$ | $R_3$ | $R_L$ | / |
| **Parameter Values** | 47.37nF | 0.046837Ω | 0.02Ω | 0.00842Ω | 50Ω or 25Ω | / |

Based on the above parameters, the mutual inductance between the two coils is measured, as shown in figure 6.

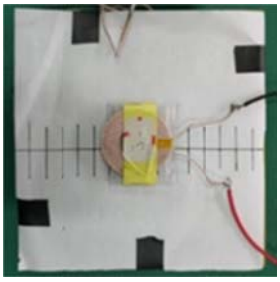

**Figure 6.** Mutual inductance measurement between two coils

Combining the results with RLS algorithm and importing the data into the program, we can get that the $M$ of the two coils is stable at 7.094 μH.

For the actual $M$ between the primary coil $L_1$ and the secondary coil $L_2$, it is impossible to get the exact value, but the "Series Decoupling" method can be used to calculate the very similar value.

The measured value of $M$ between primary and secondary coils is 6.78μH by the above method, and the error between the measured value and the experimental value of 7.094μH is about 4.626%. The error is less than 5%, it is not very large. So it is feasible to monitor the mutual inductance between coils only by measuring the DC side voltage and current of the primary side, and the accuracy is relatively high, which is basically consistent with the simulation results.

The comparison diagrams between the recursive estimates of mutual inductance, the stability values and the measured values are shown in figure 7.

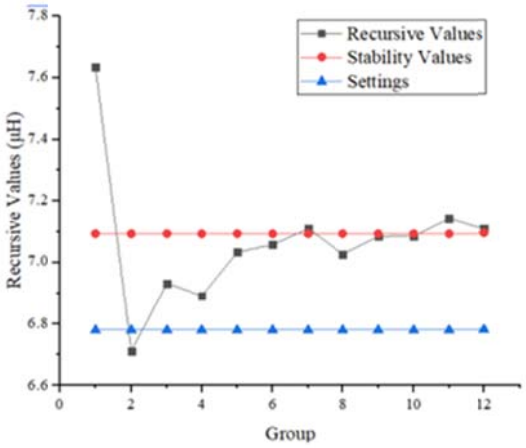


**Figure 7.** Comparisons among Recursive Values, Stable Values and Settings of Mutual Inductance

## 5. Conclusion

In this paper, through research and design, the key electrical parameters of the primary side which can reflect the overall parameters of the system are found. Thus, the key electrical parameters of the primary side can be adjusted timely and accurately according to the changes of the electrical parameters corresponding to the secondary side. The monitoring of the electrical parameters of the RMC WPT device is realized. The experimental results show that the error is within the allowable range, the accuracy of the RLS algorithm is higher, and the convergence speed is faster. Therefore, the safe operation and coordinated control of RMC WPT system are greatly guaranteed.

## 6. Acknowledgments

This work was supported by the Science and Technology Project of State Grid Corporation of China under Project of “Research on Wireless Charging Technology of Substation Patrol Robot Based on Magnetic Coupling Resonance”.

## 7. References

[1] A. Zaheer, H. Hao, G. A. Covic and D. Kacprzak. Investigation of Multiple Decoupled Coil Primary Pad Topologies in Lumped IPT Systems for Interoperable Electric Vehicle Charging[J]. IEEE Trans. Power Electron., vol. 30, no. 4, pp. 1937-1955, Apr. 2015.

[2] Z. Wang, Y. Li, Y. Sun, C. Tang, and X. Lv. Load detection model of voltage-fed inductive power transfer system. IEEE Trans Power Electron., vol. 28, no. 11, pp. 5233–5243, Feb. 2013.

[3] J. Yin, D. Lin, C. Lee, and S. Y. R. Hui. A systematic approach for load monitoring and power control in wireless power transfer systems without any direct output measurement. IEEE Trans. Power Electron., vol. 30, no. 3, pp. 1657–1667, Apr. 2015.

[4] Anonymous. Wireless Frequency Identification (RFID)[J]. Software, 2018, v.39; No.457 (05): 236-237.

[5] Qiang Minghui, Zhang Jing'e. Recognition and Simulation of RLS method based on MATLAB[J]. Automation and instrumentation, 2008 (6).

[6] C. Cai, J. Wang, R. Liu, Z. Fang, P. Zhang, M. Long, M. Hu, and Z. Lin, “Resonant Wireless Charging System Design for 110-kV High-Voltage Transmission Line Monitoring Equipment,” IEEE Transactions on Industrial Electronics, vol. 66, no. 5, pp. 4118–4129, 2019.

[7] J. Wang, C. Cai, L. Li, P. Zhang, Q. Liu, F. Zhang, Z. Fang, "Extended efficiency control method for WPT systems in smart grid under loose coupling extremes", IET Power Electronics, vol. 12, no. 10, pp. 2523-2533, 2019.

[8] C. Cai, J. Wang, Z. Fang, P. Zhang, M. Hu, J. Zhang, L. Li, and Z. Lin, “Design and Optimization of Load-Independent Magnetic Resonant Wireless Charging System for Electric Vehicles,” IEEE Access, vol. 6, pp. 17264–17274, 2018.